



High performance magnetocaloric perovskites for magnetic refrigeration

Bahl, Christian R. H.; Velazquez, David; Nielsen, Kaspar K.; Engelbrecht, Kurt; Andersen, Kjeld B.; Bulatova, Regina; Pryds, Nini

Published in:
Applied Physics Letters

Link to article, DOI:
[10.1063/1.3695338](https://doi.org/10.1063/1.3695338)

Publication date:
2012

Document Version
Publisher's PDF, also known as Version of record

[Link back to DTU Orbit](#)

Citation (APA):
Bahl, C. R. H., Velazquez, D., Nielsen, K. K., Engelbrecht, K., Andersen, K. B., Bulatova, R., & Pryds, N. (2012). High performance magnetocaloric perovskites for magnetic refrigeration. *Applied Physics Letters*, 100(12), 121905. <https://doi.org/10.1063/1.3695338>

General rights

Copyright and moral rights for the publications made accessible in the public portal are retained by the authors and/or other copyright owners and it is a condition of accessing publications that users recognise and abide by the legal requirements associated with these rights.

- Users may download and print one copy of any publication from the public portal for the purpose of private study or research.
- You may not further distribute the material or use it for any profit-making activity or commercial gain
- You may freely distribute the URL identifying the publication in the public portal

If you believe that this document breaches copyright please contact us providing details, and we will remove access to the work immediately and investigate your claim.

High performance magnetocaloric perovskites for magnetic refrigeration

Christian R. H. Bahl, David Velázquez, Kaspar K. Nielsen, Kurt Engelbrecht, Kjeld B. Andersen et al.

Citation: *Appl. Phys. Lett.* **100**, 121905 (2012); doi: 10.1063/1.3695338

View online: <http://dx.doi.org/10.1063/1.3695338>

View Table of Contents: <http://apl.aip.org/resource/1/APPLAB/v100/i12>

Published by the [American Institute of Physics](#).

Related Articles

Magnetic and magnetocaloric properties of ball milled Nd₅Ge₃
J. Appl. Phys. **111**, 073905 (2012)

Magnetic properties and magnetocaloric effect of La_{0.8}Ca_{0.2}MnO₃ nanoparticles tuned by particle size
J. Appl. Phys. **111**, 063922 (2012)

Tunable magnetocaloric effect near room temperature in La_{0.7-x}Pr_xSr_{0.3}MnO₃ (0.02 ≤ x ≤ 0.30) manganites
J. Appl. Phys. **111**, 063918 (2012)

Effect of microstrain on the magnetism and magnetocaloric properties of MnAs_{0.97}P_{0.03}
Appl. Phys. Lett. **100**, 112407 (2012)

The magnetic and magnetocaloric properties of NdFe_{12-x}Mox compounds
J. Appl. Phys. **111**, 07A949 (2012)

Additional information on *Appl. Phys. Lett.*

Journal Homepage: <http://apl.aip.org/>

Journal Information: http://apl.aip.org/about/about_the_journal

Top downloads: http://apl.aip.org/features/most_downloaded

Information for Authors: <http://apl.aip.org/authors>

ADVERTISEMENT



HAVE YOU HEARD?

Employers hiring scientists
and engineers trust
physicstoday JOBS



<http://careers.physicstoday.org/post.cfm>

High performance magnetocaloric perovskites for magnetic refrigeration

Christian R. H. Bahl,^{1,a)} David Velázquez,² Kaspar K. Nielsen,¹ Kurt Engelbrecht,¹ Kjeld B. Andersen,¹ Regina Bulatova,¹ and Nini Pryds¹

¹Department of Energy Conversion and Storage, Technical University of Denmark, DK-4000 Roskilde, Denmark

²Instituto de Ciencia de Materiales de Aragón (ICMA) CSIC, Universidad de Zaragoza, Plaza San Francisco, 50009 Zaragoza, Spain

(Received 10 February 2012; accepted 21 February 2012; published online 20 March 2012)

We have applied mixed valance manganite perovskites as magnetocaloric materials in a magnetic refrigeration device. Relying on exact control of the composition and a technique to process the materials into single adjoined pieces, we have observed temperature spans above 9 K with two materials. Reasonable correspondence is found between experiments and a 2D numerical model, using the measured magnetocaloric properties of the two materials as input. © 2012 American Institute of Physics. [<http://dx.doi.org/10.1063/1.3695338>]

Mixed valance manganites have recently found use in applications due to the rich physics present in these. The applications range from colossal magneto-resistance¹ to spintronics² and thus these ceramic perovskite materials have been extensively studied.³ The magnetocaloric effect, which manifests itself as a temperature change of the material upon a change of the applied magnetic field, is maximised close to the magnetic phase transition. Numerous studies of the magnetocaloric properties of perovskite ceramics have been conducted, finding a strong dependence of both the magnetic transition temperature and the size of the magnetocaloric effect on stoichiometry and the level and type of various dopants.^{4,5} Among the most promising of these ceramics, in view of application and device performance in the range of room temperature, are materials in the series $\text{La}_{2/3}(\text{Ca},\text{Sr})_{1/3}\text{MnO}_3$ (LCSM). While the adiabatic temperature change, ΔT_{ad} , is in general found to be relatively low compared to conventional metallic and intermetallic magnetocaloric materials, such as Gd, $\text{La}(\text{Fe},\text{Co},\text{Si})_{13}$, or $\text{Gd}_5\text{Si}_2\text{Ge}_2$, the high specific heat gives these materials an isothermal entropy change, Δs , which is close to that of Gd.⁶ We will show here how the ability of accurately tuning the Curie temperature by doping, coupled with the advantageous abilities of these materials to be shaped into fine structures, leads to high performance in magnetic refrigeration devices. This makes them promising materials for this technology, opening up yet another application for this class of materials. The high performance found in the experimental results is corroborated by numerical modelling results.

In the active magnetic regenerator (AMR) cycle, a porous magnetocaloric regenerator is alternately magnetised and demagnetised, e.g., by moving in and out of the magnet field source. After each movement, a heat transfer fluid is pushed through the void space in the regenerator in alternating directions. Upon performing this AMR cycle, a temperature gradient will build up across the regenerator, as heat is moved from the “cold end” to the “hot end”. The use of layered regenerators consisting of materials with different magnetic transition

temperatures has been proposed and experimentally tested in a few devices.^{7–9} The regenerators are constructed so that each material along the temperature gradient is operating close to its optimal temperature, i.e., Curie temperature. Such a design relies heavily on the ability to tune the Curie temperature as well as the ability of constructing a multiple material regenerator in a practical way. We show how the materials series $\text{La}_{2/3}(\text{Ca},\text{Sr})_{1/3}\text{MnO}_3$ and the processing route of tape casting are well suited to achieve this.

Powders of the two materials $\text{La}_{0.67}\text{Ca}_{0.2925}\text{Sr}_{0.0375}\text{Mn}_{1.05}\text{O}_3$ and $\text{La}_{0.67}\text{Ca}_{0.2850}\text{Sr}_{0.0450}\text{Mn}_{1.05}\text{O}_3$, referred to in the following as LCSM-1 and LCSM-2, respectively, were prepared by spray pyrolysis. Each of these powders was calcined at 1273 K for 2 h and suspended in a slurry with an azeotropic mixture of methylethylketone and ethanol, polyvinyl pyrrolidone and polyvinyl butyral. Using a so-called doctor blade to control the thickness, the slurries are applied from a vessel onto a moving substrate. This technique is known as tape casting and is a conventional processing route to produce thin and flat ceramic plates.¹⁰ The recently developed technique of adjacently tape casting multiple slurries into a single tape¹¹ was employed to prepare tapes with adjacent stripes of LCSM-1 and LCSM-2. The resulting tapes were sintered at 1473 K for 4 h to densities of 96% and 95% of the atomic, for LCSM-1 and LCSM-2, respectively. Platelets containing equal amounts of the two materials were laser cut to the size 40 mm × 25 mm, with the boundary between the materials in the middle of the 40 mm side. A stack of 28 such platelets with a total mass of 51.1 g was assembled according to the method described in Ref. 12, using a laser profilometer to quantify the quality of the stacking. An average platelet thickness of 0.30 ± 0.04 mm and channel thicknesses of 0.39 ± 0.10 mm were measured attesting to the good quality of the stacking.

The magnetocaloric properties ΔT_{ad} , Δs , and specific heat, c_H , were measured as a function of temperature and applied magnetic field on pieces of the sintered platelets of each of the two materials using the equipment discussed in Ref. 13. The data for the peak values and temperatures, in good correspondence with literature values,¹⁴ are given in Table I.

^{a)} Author to whom correspondence should be addressed. Electronic mail: chrh@dtu.dk.

TABLE I. Measured magnetocaloric properties of the two materials. ΔT_{ad} and Δs are reported upon magnetisation in an applied field of $\mu_0 H = 1$ T while c_H is at zero applied field.

Properties	Peak temperature	Peak value
<i>LCSM-1</i>		
ΔT_{ad}	277 K	1.30 K
Δs	275 K	$3.7 \text{ J kg}^{-1} \text{ K}^{-1}$
$c_H (H=0)$	273 K	$780 \text{ J kg}^{-1} \text{ K}^{-1}$
<i>LCSM-2</i>		
ΔT_{ad}	282 K	1.17 K
Δs	282 K	$3.5 \text{ J kg}^{-1} \text{ K}^{-1}$
$c_H (H=0)$	278 K	$750 \text{ J kg}^{-1} \text{ K}^{-1}$

The 28 plate stack was mounted as an active magnetic regenerator in a magnetic refrigeration test device at the Technical University of Denmark with a 1.1 T Halbach type permanent magnet assembly and a heat transfer fluid of water containing 20% commercial ethylene glycol being moved through the channels between the plates by way of a piston. The LCSM-2 parts of the plates are oriented toward the hot end, while the LCSM-1 parts of the plates are oriented toward the cold end. A heat exchanger in the hot reservoir of the device allows the hot end temperature to be controlled. Further details of this device and the operation of it can be found in Refs. 15 and 16 and a sketch of the device is given in Figure 1.

The utilization, ϕ , of the AMR is conventionally defined as the ratio between the thermal mass of fluid pushed through the regenerator and the thermal mass of the regenerator

$$\phi = \frac{m_f c_f}{M_s c_{H,s}}, \quad (1)$$

where m_f is the mass of the fluid pushed through in one direction, c_f is the specific heat of the fluid, M_s is the mass of the solid regenerator, and $c_{H,s}$ is the specific heat of the regenerator. As the regenerator consists of equal amounts of two materials, each with a temperature dependent specific heat,

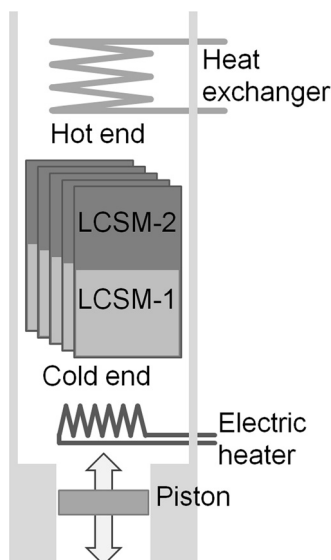


FIG. 1. Sketch of the experimental setup showing the different components.

the value chosen for $c_{H,s}$ is the average of the peak values of the two materials, i.e., $765 \text{ J kg}^{-1} \text{ K}^{-1}$. Experiments were performed with the LCSM regenerator varying the mass flow rate, the utilization, and the hot end temperature. During operation, a steady state temperature span is reached between the set hot end temperature and the cold end temperature. Figure 2(a) shows the temperature spans achieved as a function of hot end temperature and utilization, keeping the fluid flow rate at a constant value of 1.32 gs^{-1} . The highest temperature span of 9.3 K was reached at a hot end temperature of 283.8 K and a utilization of 0.4, which results in a cycle time of 8.9 s. This is an exceptionally high span, more than 7.5 times the average maximum ΔT_{ad} of the two materials. For comparison, the highest temperature span obtained in this device with of the benchmark magnetocaloric material Gd was 10.2 K,¹⁶ albeit with somewhat thicker flat plates of 0.9 mm. It is also seen that the temperature span decreases either side of the optimum utilization of 0.4, in good correspondence with previously obtained results.¹⁶ Doubling the mass flow rate while maintaining ϕ results in a lowering of the maximum temperature span to a value of 8.1 K, again at an optimum utilization of 0.4 and an optimum hot end temperature of 283.9 K. This is due to a reduction in the number of transfer units (NTU) with an increase of the mass flow rate, leading to a reduced temperature span.¹⁷

A numerical 2D model of the AMR cycle has recently been developed.¹⁸ Using only the measured properties of the LCSM plates and physical properties of the heat transfer fluid, the no-load temperature span has been modelled as shown in Fig. 2(b). Comparing the curves in Fig. 2, it is evident that the trend and peak temperatures are the same, albeit with the predicted temperature span being a little higher and

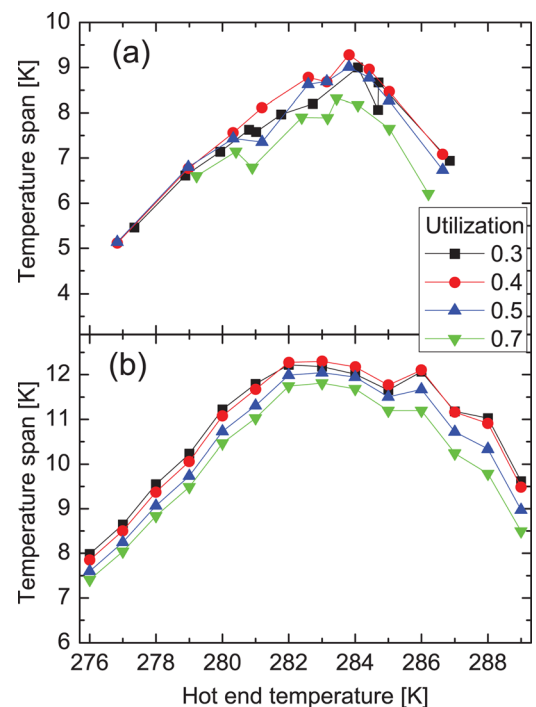


FIG. 2. (Color online) Temperature spans obtained at a mass flow rate of 1.32 gs^{-1} . (a) gives experimental results and (b) gives the predictions of the numerical model. The lines are guides to the eye.

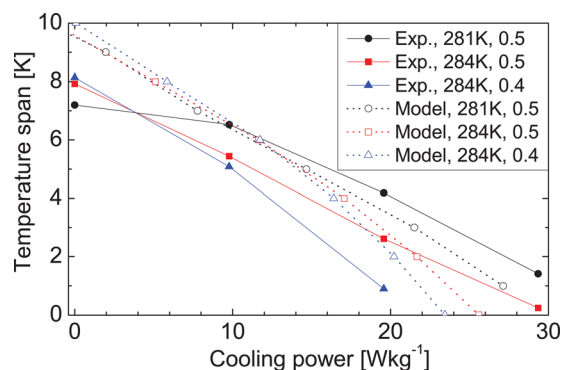


FIG. 3. (Color online) Cooling curves obtained at a mass flow rate of 2.63 gs^{-1} for both experiments and model predictions. Each curve is indexed by the hot end temperature and the utilization. The lines are guides to the eye.

the peak broader than the measured. Such a reduction in the experiment may be caused by a number of factors not accounted for in the model including thermal losses to the ambient, the effect of magnetostatic demagnetisation, and the variation of the plate spacing in the stack. Each of these factors has previously been shown to reduce the regenerator performance. Taking this into account, the correspondence seems reasonable.

Directly below the cold end of the regenerator, there is a small electrical heater. Applying power to this simulates the presence of a cooling load in the refrigeration device allowing the cooling curve to be mapped out. The cooling curves have been recorded for different utilizations and hot end temperatures keeping the mass flow rate at a constant value. Depending on the device performance, there will be a variation in the heat transfer between the heat exchanger and the hot end of the device. This results in a slight variation ($\sim 0.2 \text{ K}$) in the actual hot end temperature at a fixed set-point temperature, so for comparison rounded values of the hot end temperature are reported.

The best performance is observed at a mass flow rate of 2.63 gs^{-1} and Figure 3 shows the results, with the cooling power normalised to the mass of the regenerator for convenience. At zero load, the highest span is, as discussed above, at a utilization of 0.4 and a hot end of 284 K. As expected, the span is reduced as the load increases. This decrease is close to linear for single material regenerators^{8,17} and for two material regenerators with a close spacing of Curie temperatures.⁹ An increase in the maximum cooling power is observed when the utilization is increased to 0.5, due to the increased thermal capacity of the fluid being pushed through the regenerator. Also, the lower span at high cooling power favours the lower hot end temperature of 281 K as this brings the temperature span closer to the range where both LCSM materials operate best. Figure 3 also gives the results from the numerical model. Again, the trends are observed to be the same with regards to the order and crossing of the lines. As expected, the model over predicts the temperature span, but surprisingly the experimental zero span cooling powers are slightly above the predicted values. This may be caused by dissipation of some of the heater power through the walls of the device rather than into the regenerator. The extrapo-

lated maximum zero-span cooling power of about 35 W kg^{-1} in the experiment is significantly larger than the highest measured value of 16 W kg^{-1} for Gd plates in the same device in similar conditions.¹⁹ Due to the lower parasitic loss of larger devices and the faster operation possible when using packed bed regenerators, significantly higher values are reported for such devices^{8,9} but at the cost of a significantly higher pumping pressure.

In conclusion, the results clearly show the potential value of the mixed valence manganese ceramics as magnetocaloric materials for application in devices. The strength of the materials lies in the ability to accurately tune the Curie temperature and process the materials into thin plates with adjacent regions of different Curie temperatures. Future regenerators will be constructed of numerous adjacent materials, leading to further improvements of the performance. The relatively low cost of materials and especially the processing route, compared to conventional materials and processing routes, reduces the price which is otherwise a major obstacle in the way of magnetocaloric applications.

The authors would like to acknowledge the support of the Programme Commission on Energy and Environment (EnMi) (Contract No. 2104-06-0032) which is part of the Danish Council for Strategic Research.

- ¹S. Jin, T. H. Tiefel, M. McCormack, R. A. Fastnacht, R. Ramesh, and L. H. Chen, *Science* **264**, 413 (1994).
- ²J.-H. Park, E. Vescovo, H.-J. Kim, C. Kwon, R. Ramesh, and T. Venkatesan, *Nature* **392**, 794 (1998).
- ³J. M. D. Coey, M. Viret, and S. von Molnár, *Adv. Phys.* **58**, 571 (2009).
- ⁴M.-H.-H. Phan and S.-C.-C. Yu, *J. Magn. Magn. Mater.* **308**, 325 (2007).
- ⁵K. A. Gschneidner, Jr., V. K. Pecharsky, and A. O. Tsokol, *Rep. Prog. Phys.* **68**, 1479 (2005).
- ⁶K. A. Gschneidner, Jr. and V. K. Pecharsky, *Annu. Rev. Mater. Sci.* **30**, 387 (2000).
- ⁷A. Rowe and A. Tura, *Int. J. Refrig.* **29**, 1286 (2006).
- ⁸S. Russek, J. Auringer, A. Boeder, J. Chell, S. Jacobs, and C. Zimm, in *Proceedings of the 4th International Conference on Magnetic Refrigeration at Room Temperature, Baotou, Inner Mongolia, China* (International Institute of Refrigeration, Paris, France, 2010), p. 339.
- ⁹D. Arnold, A. Tura, and A. Rowe, *Int. J. Refrig.* **34**, 178 (2011).
- ¹⁰A. Larbot, *Fundamentals of Inorganic Membrane Science and Technology, Membrane Science and Technology*, Vol. 4, edited by A. Burggraaf and L. Cot (Elsevier Science B.V., Amsterdam, The Netherlands, 1996) pp. 119–139.
- ¹¹R. Bulatova, K. B. Andersen, L. Theil Kuhn, C. R. H. Bahl, and N. Pryds, Adjacent tape casting of multiple ceramic slurries, (unpublished).
- ¹²K. Engelbrecht, K. K. Nielsen, and N. Pryds, *Int. J. Refrig.* **34**, 1817 (2011).
- ¹³R. Bjørk, C. R. H. Bahl, and M. Katter, *J. Magn. Magn. Mater.* **322**, 3882 (2010).
- ¹⁴A. R. Dinesen, S. Linderoth, and S. Mørup, *J. Phys.: Condens. Matter* **17**, 6257 (2005).
- ¹⁵C. R. H. Bahl, T. F. Petersen, N. Pryds, and A. Smith, *Rev. Sci. Instrum.* **79**, 093906 (2008).
- ¹⁶K. Engelbrecht, C. R. H. Bahl, and K. K. Nielsen, *Int. J. Refrig.* **34**, 1132 (2011).
- ¹⁷K. K. Nielsen, C. R. H. Bahl, A. Smith, N. Pryds, and J. H. Hattel, *Int. J. Refrig.* **33**, 753 (2010).
- ¹⁸K. K. Nielsen, C. R. H. Bahl, A. Smith, R. Bjørk, N. Pryds, and J. H. Hattel, *Int. J. Refrig.* **32**, 1478 (2009).
- ¹⁹K. K. Nielsen, R. Bjørk, J. B. Jensen, C. R. H. Bahl, N. Pryds, A. Smith, A. Nordentoft, and J. Hattel, in *Proceedings of the 8th IIF/IIR Gustav Lorentzen Conference on Natural Working Fluids, Copenhagen, Denmark, September 7-10, 2008*.